

Penetration effect of connected and automated vehicles on cooperative on-ramp merging

Jishiyu Ding¹, Huei Peng², Yi Zhang³, Li Li³ ✉

¹Department of Automation, Tsinghua University, Beijing 100084, People's Republic of China

²Department of Mechanical Engineering, University of Michigan, Ann Arbor, MI 48109, USA

³Department of Automation, BNRist, Tsinghua University, Beijing 100084, People's Republic of China

✉ E-mail: li-li@tsinghua.edu.cn

ISSN 1751-956X

Received on 24th July 2019

Revised 13th September 2019

Accepted on 10th October 2019

E-First on 5th December 2019

doi: 10.1049/iet-its.2019.0488

www.ietdl.org

Abstract: Earlier work has established a centralised cooperative merging framework of optimally coordinating two strings of connected and automated vehicles (CAVs) passing through the on-ramp merging zone. The proposed merging strategy is capable of making a good trade-off between performance and computational cost. In this study, the authors address the problem of optimally coordinating CAVs under mixed traffic conditions, where both CAVs and human-driven vehicles (non-CAVs) travel on the roads, so as to enhance efficiency while guaranteeing safety constraints. A hierarchical cooperative merging framework is proposed for CAVs, which integrates merging sequence scheduling strategies (high level) and motion planning methods (low level). The impacts of CAV penetration (i.e. the fraction of CAVs relative to all vehicles) on throughput, delay, fuel consumption and emission are also investigated under different traffic demands. Simulation-based case studies indicate that the performance improvement becomes more significant as the CAV penetration rate increases and about 30% CAV penetration can effectively mitigate the shockwave and reduce traffic congestion.

1 Introduction

Driving on highways is usually safe, and one of the most challenging scenarios involving speed modulation is highway on-ramps. A basic method that improves safety and efficiency is ramp metering [1]. There have been many ramp metering approaches developed to improve both safety and throughput [2–4]. With the development of vehicle-to-vehicle (V2V) and vehicle-to-infrastructure (V2I) technologies, connected and automated vehicles (CAVs) can improve safety and efficiency by information sharing and vehicle coordination [5]. Several novel approaches to address traffic congestion caused by merging roadways have been considered. In these efforts, it is assumed that the vehicles are connected by V2V communication and their speed can be manipulated. Safe and efficient coordination is then possible [6].

Our earlier work [7] has established a centralised cooperative merging framework for coordinating two strings of CAVs passing through the merging zone effectively and safely. In our approach, the rule-based merging strategy computes a near-optimal merging sequence in terms of travel delay and safety, and the motion planning algorithm is designed for energy-saving. We also validate the effectiveness and robustness of the cooperative merging strategy under both balanced and unbalanced traffic scenarios through simulation.

The benefits of CAV coordination and control on traffic efficiency have been established and quantified in recent literature [5]. However, the pure CAV environment seems to be not possible in the few decades and the integration of CAVs with human-driven vehicles (non-CAVs) faces several challenges before their penetration rate (i.e. the fraction of CAVs relative to all vehicles in a transportation system) becomes significant. The management of mixed traffic scenario (i.e. both human-driven vehicles and CAVs on the road) is an inevitable problem during the process of CAV development. Thus, a critical question is investigating the penetration effect of CAVs under mixed traffic conditions. It is beneficial to the promotions and applications of CAVs by understanding their penetration effect, which helps us to find a transitional solution under mixed traffic [8].

Rule-based methods [9] and optimisation-based methods [10, 11] for the merging scenario with 100% CAV penetration are both

explored in the literature. A survey of the research efforts in this area that have been reported in the literature to date can be found in [12]. Under mixed traffic conditions, it is necessary to design coordination policies that can accommodate both CAVs and conventional human-driven vehicles. Under mixed traffic environment, the cooperative merging strategies can be generally grouped into three categories: rule-based methods, optimisation-based methods and learning-based methods. However, there is usually a trade-off between computation load and optimality. Determining the merging sequence using rule-based approaches is computationally efficient but not optimal. For optimisation-based and learning-based approaches, the main challenge lies in finding an optimal merging sequence with large number of vehicles in real time.

To address the aforementioned problems, a hierarchical cooperative merging framework shown in Fig. 1 is proposed to investigate the penetration effect. In the high level, the merging sequence of vehicles can be optimised, which can be generalised into four cases: full coordination, partial coordination, adaptive following and no coordination. Different cases can be chosen according to whether the newly detected vehicle and its surrounding vehicles are CAVs or not. In the case of non-CAVs, we also design appropriate merging strategies to model human-like merging behaviours. In the low level, two different energy-efficient motion planning modes, namely free driving mode and adaptive cruising mode, are designed for CAVs and Gipps car-following model is utilised to model the behaviours of non-CAVs.

In our approach, the merging sequence scheduling level coordinates CAVs in terms of efficiency as well as safety, and the motion planning methods are designed for energy saving. Analysis and simulation results show that the traffic congestion can be mitigated by a certain penetration of CAVs and the improvement on performances becomes more significant with the increase of CAV penetration. The main contributions of this work are summarised as follows:

- To optimise the merging sequence of vehicles, a hierarchical framework of cooperative merging is proposed under mixed traffic environment.

- To investigate the penetration effect, both microscopic impact (e.g. vehicle trajectories) and macroscopic impact (e.g. throughput, delay and fuel consumption) are taken into consideration.

To give a better presentation of our findings, the rest of the paper is organised as follows. Section 2 briefly reviews the recent studies on cooperative merging under mixed traffic environment. Section 3 reviews the cooperative merging problem at highway on-ramps. Section 4 presents the cooperative merging framework for CAVs, while Section 5 introduces the car-following model and merging framework for human-driven vehicles. Simulation-based case studies are carried out in Section 6. Finally, concluding remarks are given in Section 7.

2 Related works

To the best of our knowledge, there are a few studies that investigate the impact of the CAV penetration on traffic flow characteristics in the on-ramp merging scenario and these studies can be generally grouped into three categories: rule-based methods, optimisation-based methods and learning-based methods.

2.1 Rule-based methods

Zhang and Cassandras [13] proposed a vehicle coordination algorithm base on the ‘first-in-first-out’ (FIFO) rule in signal-free intersections and validated the energy benefits of CAVs, while Zhao *et al.* [14] adopted the similar idea in roundabouts. However, no consideration was given to the microscopic performances (e.g. vehicle trajectories) and macroscopic performances (e.g. throughput, delay and ride comfort). Zou and Qu [15] proposed a cooperative cellular automata model to investigate the impact of CAVs in freeway work zones, which is similar to the on-ramp merging scenario. Zhou *et al.* [16] and Park *et al.* [17] utilised a modified Intelligent Driver Model to reduce the total travel time and smooth traffic oscillations. Han and Ahn [18] proposed a Variable Speed Release control policy to increase bottleneck capacity, while Davis [19] investigates the penetration effect of adaptive cruise control systems on mixed traffic flow. However, these kinds of studies utilised a simple rule-based method for merging logic and did not optimise the merging sequence of vehicles.

2.2 Optimisation-based methods

Rios-Torres and Malikopoulos [20, 21] investigated the impact of partial penetrations of CAVs on fuel consumption and traffic flow. Bai *et al.* [22] proposed a cooperative weaving motion planner for CAVs to reduce traffic oscillation based on model predictive control (MPC) method in weaving areas. However, these studies only optimised the vehicle trajectories and assumed that the merging sequences of vehicles are fixed, which are *ad hoc* and their optimality cannot be guaranteed. Xie *et al.* [23] proposed a collaborative merging assistance method for on-ramp CAVs. The proposed ramp control strategy is a constrained non-linear optimisation problem which provides individual vehicles with step-by-step control instruction. Letter and Elefteriadou [24] proposed a trajectory optimisation algorithm to maximise the average vehicle speed on the ramp and the target lane. Among these optimisation-based studies, the main issues lie in ignoring the merging sequence scheduling and solving the complicated optimisation problem in real time.

2.3 Learning-based methods

Vinitsky *et al.* [25] proposed a merging strategy via reinforcement learning to control shockwaves from on-ramp merges. Furthermore, they showed the ability of learning-based methods to enhance traffic efficiency in some other scenarios by learning the optimal policies for CAVs. Kreidieh *et al.* [26] proposed a deep reinforcement learning framework for cooperative merging problems to dissipate the stop-and-go waves caused by merging behaviours. Most of the learning-based methods try to maximise the number of vehicles that pass through the network and do not take the microscopic impacts into consideration.

As aforementioned, there is usually a trade-off between computation load and optimality and few studies investigate both the microscopic and macroscopic impacts of CAV penetrations. Therefore, a hierarchical cooperative merging framework is proposed to investigate the penetration effect under mixed environment.

3 Problem description

This paper focuses on investigating the impacts of CAV penetration on the on-ramp merging process. The objective is to coordinate all the vehicles passing the merging zone safely and efficiently and to

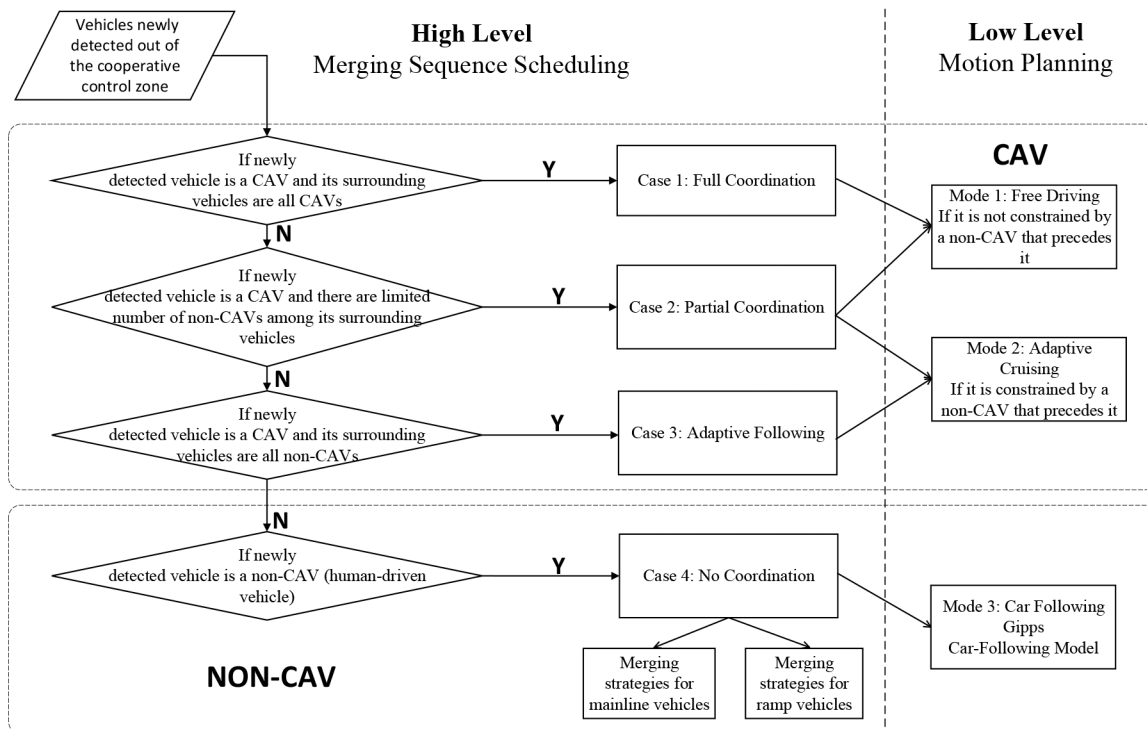


Fig. 1 Hierarchical framework of cooperative merging

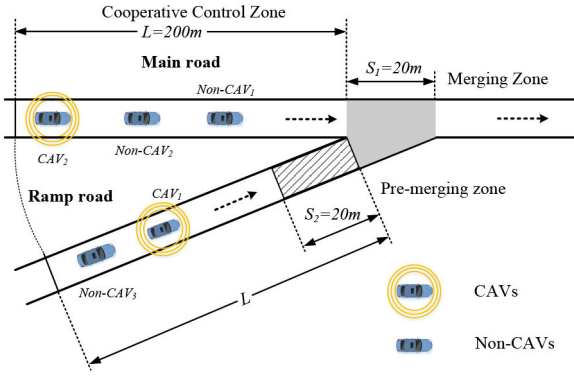


Fig. 2 Diagram of vehicle cooperative merging problem

Table 1 Variables and definitions

Variable	Definition
L	length of the cooperative control zone
S_1	length of the merging zone
S_2	length of the pre-merging zone
v_i	velocity of vehicle i
p_i	position of vehicle i
a_i	acceleration or deceleration of vehicle i
v_{\min}, v_{\max}	minimum and maximum velocities of a vehicle
a_{\min}, a_{\max}	minimum and maximum accelerations of a vehicle
Δt_1	minimum safety headway in the same leg
Δt_2	minimum safety headway in different legs
t_{assign}^i	assigned arrival time of vehicle i
t_{\min}^i	minimum arrival time of vehicle i

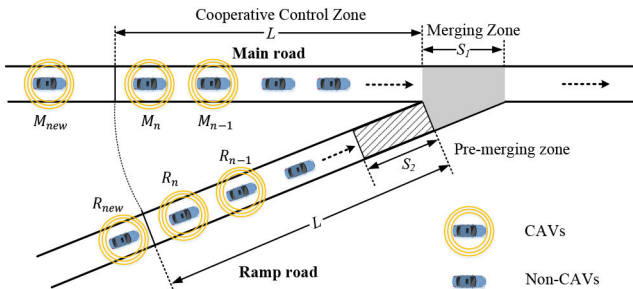


Fig. 3 Diagram of full coordination mode

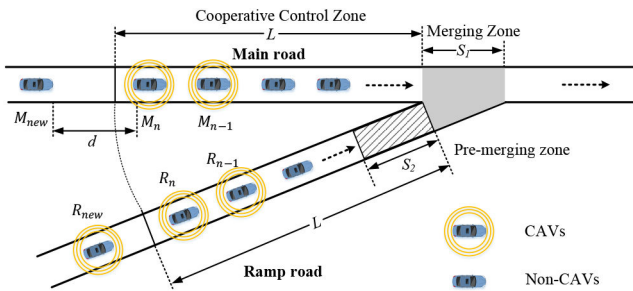


Fig. 4 Diagram of partial coordination mode

mitigate the stop-and-go operations under mixed traffic conditions, where both CAVs and human-driven vehicles (non-CAVs) travel on the roads. We briefly review the model introduced in [7], where there are two legs, mainline and ramp road, illustrated in Fig. 2. The region in a shaded area, called merging zone, is the area of potential lateral collision. In addition, there is a region in the dash area, called pre-merging zone, is the area where non-CAVs begin the merging process. There is also a cooperative control zone where CAVs begin the cooperative merging process.

In the model described above, we impose the following assumptions: (i) only the rightmost lane of highway is taken into account for on-ramp merging, and the on-ramp only has one lane, (ii) non-CAVs on-ramp can observe and interact with mainline vehicles within the pre-merging zone, (iii) each connected and automated vehicle has proximity sensors and can measure local information without errors or delays, such as the velocity and position of the preceding non-CAV, (iv) only the longitudinal control is considered in this study, while default lane change models are used for the lateral control.

Table 1 summarises some of the major variables and corresponding definitions used in this paper.

In our previous approach [7], the proposed cooperative merging strategy computes a near-optimal merging sequence in real time in terms of travel delay and safety, and the motion planning algorithm is designed for energy saving. The extended cooperative merging frameworks under mixed traffic scenario are presented in the following sections.

4 Cooperative merging framework for CAVs

A hierarchical cooperative merging framework for CAVs shown in Fig. 1 is proposed under the mixed traffic scenario, which integrates merging sequence scheduling strategies and motion planning methods.

4.1 Merging sequence scheduling strategies for CAVs

Under mixed traffic scenario, merging sequence scheduling strategies for CAVs can be generalised into three cases: (i) full coordination when the surrounding vehicles of newly detected CAVs are all CAVs (ii) partial coordination when there are a limited number of non-CAVs among the surrounding vehicles and (iii) adaptive following when the surrounding vehicles are all non-CAVs.

4.1.1 Case 1: full coordination: If the surrounding vehicles of newly detected CAVs (e.g. M_{new} and R_{new} in Fig. 3) are all CAVs, the assigned arrival time of newly detected CAVs can be determined through the merging sequence adjustment algorithm in [7], where the rule-based cooperative merging strategy achieves a near-optimal solution of the merging sequence. It should be noted that full coordination cases may only occur under high CAV penetration scenarios.

4.1.2 Case 2: partial coordination: Since human-driven vehicles (non-CAVs) cannot be coordinated, partial coordination will be carried out under mixed traffic scenarios. It should be noted that the position and velocity of a non-CAV can be measured by a preceding or following CAV through on-board sensors. Based on the local information measured by CAVs, the newly detected CAVs can be coordinated to avoid stop-and-go operations during the merging process. An example in Fig. 4 is utilised to illustrate this. In this example, the merging sequence of the vehicles inside the cooperative control zone is assumed to be determined by our previous approach already [7] and the vehicle M_n is the last one in the sequence. The merging sequence of CAV R_{new} and non-CAV M_{new} depends on the inter-vehicle distance between vehicle M_{new} and vehicle M_n . If the inter-vehicle distance d is large enough, CAV R_{new} should be coordinated to arrive at the merging zone earlier than the non-CAV M_{new} . Otherwise, CAV R_{new} should be coordinated to arrive at the merging zone after non-CAV M_{new} to avoid stop-and-go operations. The details of the partial coordination algorithm are presented as follows.

Since CAVs cannot communicate with non-CAVs, they simply assume a constant speed for non-CAVs to estimate their arrival time. Thus, the estimated arrival time at the merging zone can be calculated by (1). Note that the estimation may need re-evaluation in the case that non-CAVs change speed

$$t_{\text{in}}^{M_{\text{new}}} = t_0 + \frac{L - p_{M_{\text{new}}}(t_0)}{v_{M_{\text{new}}}(t_0)} \quad (1)$$

where $\hat{t}_{in}^{M_{new}}$ is the estimated arrival time at the merging zone of newly detected mainline vehicle M_{new} , $p_{M_{new}}(t_0)$ and $v_{M_{new}}(t_0)$ are the position and velocity of the vehicle M_{new} at time t_0 .

Thus, the CAV R_{new} is assigned to arrive the merging zone later than the non-CAV M_{new} if the inter-vehicle distance d is not long enough, which satisfies (2) and the assigned arrival time can be calculated by (3). Otherwise, CAV R_{new} can be assigned to arrive at the merging zone between non-CAV M_{new} and CAV M_n and the assigned arrival time can be calculated by (4)

$$d \leq v_{R_{new}} \Delta t_2 + v_{M_{new}} h_d \quad (2)$$

where d is the distance between non-CAV M_{new} and CAV M_n , $v_{R_{new}} \Delta t_2$ refers to the virtual desired headway between CAV R_{new} and CAV M_n , $v_{M_{new}} h_d$ refers to the virtual desired headway between CAV R_{new} and non-CAV M_{new}

$$t_{assign}^{R_{new}} = \max \left\{ \hat{t}_{in}^{M_{new}} + \Delta t_2, t_{min}^{R_{new}} \right\} \quad (3)$$

$$t_{assign}^{R_{new}} = \max \left\{ t_{assign}^{M_n} + \Delta t_2, t_{min}^{R_{new}} \right\} \quad (4)$$

where $t_{assign}^{R_{new}}$ is the assigned arrival time at the merging zone of newly detected ramp CAV, $t_{min}^{R_{new}}$ is the minimum arrival time of CAV R_{new} and $t_{assign}^{M_n}$ is the assigned arrival time at the merging zone of the vehicle M_n .

In order to avoid assigning unrealistic arrival time to the vehicles, we need to calculate the minimum arrival time. Namely, vehicles first accelerate to the maximum velocity and then cruise to the merging zone. The calculation is based on the basic kinematics and readers can refer to [7].

The details of the partial coordination strategy are included in Algorithm 1 (see Fig. 5).

4.1.3 Case 3: adaptive following: When the surrounding vehicles of newly detected CAVs (e.g. R_{new} in Fig. 6) are all non-CAVs, the newly detected CAVs could only execute the adaptive following action, which is constrained by the preceding non-CAVs. Since we cannot get information about non-CAV M_{new} , the

Inputs: $v_{R_{new}}, v_{M_{new}}, p_{M_{new}}$
Outputs: $t_{assign}^{R_{new}}$
1 : Calculate inter-vehicle distance d between non-CAV M_{new} and CAV M_n
2 : if $d \leq v_{R_{new}} \Delta t_2 + v_{M_{new}} h_d$
3 : Assign the CAV R_{new} arriving at the merging zone later than the non-CAV M_{new}
4 : Calculate the assigned arrival time of CAV R_{new} using Eq. (3)
5 : else
6 : Assign the CAV R_{new} arriving at the merging zone earlier than the non-CAV M_{new}
7 : Calculate the assigned arrival time of CAV R_{new} using Eq. (4)
8 : end if

Fig. 5 Algorithm 1: Partial coordination algorithm for CAVs

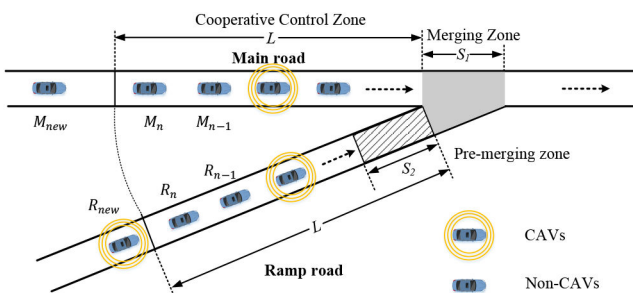


Fig. 6 Diagram of the adaptive following mode

assigned arrival time for newly detected ramp CAV R_{new} can be only determined by estimating the arrival time of the preceding vehicle R_n as shown in Fig. 6

$$t_{assign}^{R_{new}} = \max \left\{ \hat{t}_{in}^{R_n} + \Delta t_1, t_{min}^{R_{new}} \right\} \quad (5)$$

$$\hat{t}_{in}^{R_n} = t_0 + \frac{L - p_{R_n}(t_0)}{v_{R_n}(t_0)} \quad (6)$$

where $\hat{t}_{in}^{R_n}$ is the estimated arrival time at the merging zone of ramp non-CAV R_n .

4.2 Motion planning methods for CAVs

In terms of a CAV, there are two driving modes that it can be in (i) free driving (FD mode) when it is not constrained by a non-CAV that precedes it, and (ii) adaptive cruising (AC mode) when it follows a preceding non-CAV while adaptively maintaining a safe distance from it. CAVs will switch from the FD mode to the AC mode as soon as the inter-vehicle distance falls below a certain threshold. It should be noted that the virtual vehicle mapping method [6] is used as a benchmark to show the benefits of energy saving.

A linear model for vehicle longitudinal dynamics is utilised to describe the dynamics of CAVs

$$\dot{x}_i(t) = Ax_i(t) + Bu_i(t) \quad (7)$$

where

$$x_i(t) = \begin{bmatrix} p_i \\ v_i \\ a_i \end{bmatrix}, \quad A = \begin{bmatrix} 0 & 1 & 0 \\ 0 & 0 & 1 \\ 0 & 0 & -\frac{1}{\tau} \end{bmatrix}, \quad B = \begin{bmatrix} 0 \\ 0 \\ \frac{1}{\tau} \end{bmatrix},$$

p_i, v_i and a_i denote the position, velocity and acceleration of the vehicle i , respectively, and τ denotes the first-order inertial constant.

4.2.1 Free driving mode: In this mode, the objective of each CAV is to derive an optimal acceleration/deceleration profile, in terms of minimising the energy consumption inside the cooperative zone. The energy-efficient motion planning method can be formulated as a convex optimisation problem written as (8), which tries to minimise the accelerations or decelerations during the merging process.

$$\begin{aligned} \min_{a_i} \quad & \frac{1}{2} \int_{t_0}^{t_{assign}^i} a_i^2(t) dt \\ \text{s.t.} \quad & v_{min} \leq v_i \leq v_{max} \\ & a_{min} \leq a_i \leq a_{max} \end{aligned} \quad (8)$$

where t_0 is the initial time, t_{assign}^i is the assigned arrival time.

An analytical solution to the above problem can be obtained through a Hamiltonian analysis found in [7]. Consequently, the optimal control input (acceleration/deceleration) as a function of time is given by

$$a_i^*(t) = b_i t + c_i \quad (9)$$

where b_i and c_i are constants which can be computed online.

4.2.2 Adaptive cruising mode: When the inter-vehicle distance between CAV i and the preceding non-CAV $i-1$ falls below a certain threshold ΔL , CAV i switches from the FD mode to the AC mode. In this mode, the objective of each CAV is to derive an optimal acceleration/deceleration profile so as to minimise fuel

Inputs: $v_{i-1}(t), p_{i-1}(t), v_i(t), p_i(t)$
Outputs: $a_i(t + \tau), v_i(t + \tau), p_i(t + \tau)$
1: if the mainline non-CAV does not reach the merging zone
2: Consider its preceding vehicle as its leading vehicle
3: Use Gipps model to compute $a_i(t + \tau), v_i(t + \tau), p_i(t + \tau)$
4: else
5: if there exists a vehicle on the ramp road merging into mainline
6: Consider the merging vehicle as a new leading vehicle
7: else
8: Continue following the preceding mainline vehicle
9: end if
10: Use Gipps model to compute $a_i(t + \tau), v_i(t + \tau), p_i(t + \tau)$
11: end if

Fig. 7 Algorithm 2: Merging algorithm for mainline non-CAVs

consumption, while maintaining the minimum safe following distance with the preceding non-CAV:

$$\min_{a_i} \frac{1}{2} \int_{t_0}^{t_{\text{assign}}} [\omega_1 a_i(t)^2 + \omega_2 (p_i(t) - p_{i-1}(t) - \Delta L)^2] dt \quad (10)$$

$$\text{s.t. } v_{\min} \leq v_i \leq v_{\max}$$

$$a_{\min} \leq a_i \leq a_{\max}$$

where ω_1 and ω_2 are weights applied to the objective function, which allows trading off energy consumption minimisation against maintaining the safe following distance, ΔL is the minimum safe following distance between CAV i and the preceding non-CAV $i - 1$.

The analytical solution of problem (10) can be obtained through a Hamiltonian analysis similar to that in [13]. Defining $\omega = \sqrt{4\omega_1\omega_2}/2\omega_1$ and $\alpha = \sqrt{\omega}/2$, the optimal control can be obtained as follows:

$$a_i^*(t) = -2b_i\alpha^2 e^{\alpha t} \sin(\alpha t) + 2c_i\alpha^2 e^{-\alpha t} \sin(\alpha t) + 2d_i\alpha^2 e^{\alpha t} \cos(\alpha t) - 2e_i\alpha^2 e^{-\alpha t} \cos(\alpha t) \quad (11)$$

where b_i, c_i, d_i and e_i are constants of integration, which can be obtained in a similar way as (9).

5 On-ramp merging framework for non-CAVs

There are two major issues that need to be addressed for non-CAVs under mixed traffic scenarios: (i) modelling the car-following behaviour for human-driven vehicles, and (ii) designing a human-like merging strategy to avoid collision in the merging zone.

5.1 Car-following model

Gipps car-following model [27] is utilised to describe the behaviours of non-CAVs, which aims to keep a safe following distance from the leading vehicle or to travel at the desired speed in free traffic flow. According to our simulation results, it should be noted that the selection of car-following model has little impact on the cooperative merging performances.

According to Gipps model, the speed of the following vehicle can be computed as follows:

$$v_i(t + \tau) = \min \{v_{i,\text{acc}}(t + \tau), v_{i,\text{dec}}(t + \tau)\} \quad (12)$$

$$v_{i,\text{acc}}(t + \tau) = v_i(t) + 2.5 \times a_{\max} \times \tau \times \left(1 - \frac{v_i(t)}{v_{\max}}\right) \times \sqrt{0.025 + \frac{v_i(t)}{v_{\max}}} \quad (13)$$

$$v_{i,\text{dec}}(t + \tau) = a_{\max} \tau + \left\{ a_{\min}^2 \tau^2 - a_{\min} [2(p_{i-1}(t) - p_i(t) - L_{\text{veh}} - L_d) - v_i(t)\tau - \frac{v_i(t)}{a_{\min}}] \right\}^{1/2} \quad (14)$$

where the subscripts $i, i - 1$ denote the following and the leading vehicles, respectively, τ denotes the reaction time of drivers, $v_{i,\text{acc}}(t + \tau), v_{i,\text{dec}}(t + \tau)$ represent the updated velocity of the following vehicle in free-flow and congested conditions, respectively, L_{veh} is the length of vehicle and L_d is the desired headway distance when the vehicles are at stop.

5.2 Merging strategies for non-CAVs

In this subsection, merging strategies for human-driven vehicles (non-CAVs) [20] on both mainline and ramp road are adopted to model the human-like merging behaviours and to avoid a lateral collision in the merging zone, which are also in compliance with the traffic regulations.

5.2.1 Merging strategy for mainline non-CAVs: A vehicle travelling on the main road will consider its preceding vehicle as its leader and will follow the speed dictated by the Gipps model until it reaches the merging zone. Once in the merging zone, the vehicle will evaluate whether there is a vehicle merging in front; in such case, it will start considering the merging vehicle as its new leader. The details of the strategy are included in Algorithm 2 (see Fig. 7).

5.2.2 Merging strategy for ramp road non-CAVs: A vehicle travelling on the ramp road will consider its preceding vehicle on the road as its leader until it reaches the pre-merging zone. Once there, the ‘driver’ starts evaluating the merging conditions and looks for the closest safe gap to merge by choosing a new potential leader and a new potential follower in the main road. If the estimated time headways among them are less than a certain threshold, the ramp vehicle will start decelerating to be able to stop and avoid a lateral collision. The ‘driver’ will then wait until the next available gap to evaluate the merging conditions again. Once the vehicle merges, it will continue following the speed dictated by the Gipps car-following model to try to keep a safe distance from its new leader on the main road.

The estimated time headway among them can be calculated as (15) and (16). The details of the strategy are included in Algorithm 3 (see Fig. 8)

$$t_{\text{gap1}} = \frac{p_i(t) - p_r(t)}{v_r(t)} \quad (15)$$

$$t_{\text{gap2}} = \frac{p_r(t) - p_{i-1}(t)}{v_{i-1}(t)} \quad (16)$$

where the subscripts $i, i - 1$ and r denote the mainline potential leader, mainline potential follower and ramp vehicle preparing to merge, respectively, t_{gap1} denotes the virtual time headway between potential leader and ramp vehicle, t_{gap2} denotes the virtual time headway between ramp vehicle and its potential follower.

6 Simulation results

We first perform a simple example to illustrate the partial coordination logic among CAVs and non-CAVs as well as its microscopic impact on traffic flow. Subsequently, to evaluate the robustness of the proposed method and its macroscopic impact on traffic flow (i.e. throughput and delay), the proposed cooperative merging strategy is implemented under mixed traffic scenarios. Three cases are taken into consideration, namely, no CAV penetration, partial CAV penetration and full CAV penetration. In the case of no CAV penetration, all the vehicles entering the cooperative control zone behave according to the Gipps car-following model and use the merging framework for non-CAVs to pass the merging zone. In the case of partial CAV penetration, the Gipps car-following model and the cooperative merging framework are combined to guide vehicles during the merging process. In the third case, all CAVs will be coordinated according to the rule-based cooperative merging strategy in [7] to pass the merging zone. Thus, to explore the effects of gradual penetration of

CAVs, penetration rates of CAVs range from 0 to 100%, with an interval of 10%.

Inputs:	$v_{i-1}(t), p_{i-1}(t), v_i(t), p_i(t), v_r(t), p_r(t)$
Outputs:	$a_i(t + \tau), v_i(t + \tau), p_i(t + \tau)$
1:	if the ramp non-CAV does not reach the pre-merging zone
2:	Consider its preceding vehicle as its leading vehicle
3:	Use Gipps model to compute $a_i(t + \tau), v_i(t + \tau), p_i(t + \tau)$
4:	else if the ramp non-CAV drives in the pre-merging zone
5:	if there exists a gap available in the mainline: $t_{gap} \geq 1.5s$
6:	Choose a new potential leader and a new potential follower in the main road;
7:	else
8:	Start decelerating to stop before entering in the merging zone;
9:	Wait until the next available gap and choose a new leader;
10:	end if
11:	Use Gipps model to compute $a_i(t + \tau), v_i(t + \tau), p_i(t + \tau)$
12:	else
13:	Use Gipps model to compute $a_i(t + \tau), v_i(t + \tau), p_i(t + \tau)$
14:	end if

Fig. 8 Algorithm 3: Merging algorithm for ramp road non-CAVs

Table 2 Simulation parameters

Variable	Value
L	200 m
S_1, S_2	20 m, 20 m
ΔL	10 m
ω_1, ω_2	0.5, 0.5
v_{min}, v_{max}	0 m/s, 25 m/s
a_{min}, a_{max}	$-3 \text{ m/s}^2, 3 \text{ m/s}^2$
λ	0.1 veh/s, 0.25 veh/s
$\Delta t_1, \Delta t_2, h_d$	1 s, 1.5 s, 2 s

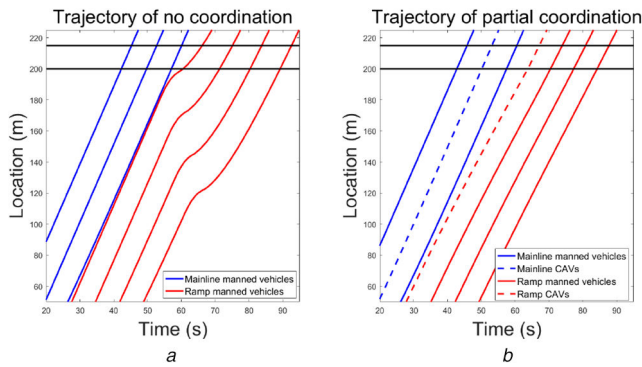


Fig. 9 Trajectory comparison of no coordination and partial coordination (a) Vehicle trajectories with no coordination, (b) Vehicle trajectories with partial coordination

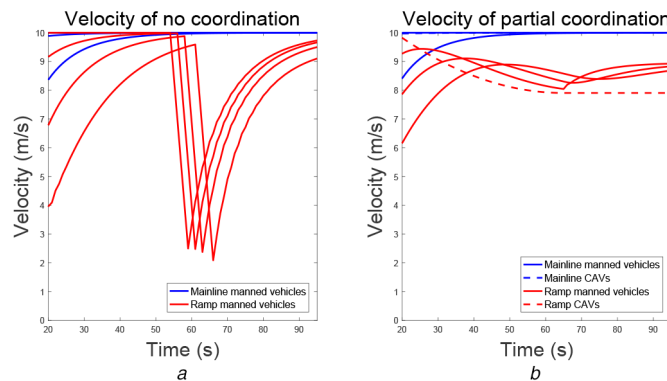


Fig. 10 Velocity profile comparison of no coordination and partial coordination (a) Velocity profiles with no coordination, (b) Velocity profiles with partial coordination

All experiments are carried out on a regular computer (operating system: Windows 10 64bit; workbench: Matlab R2017b; CPU: Intel i7-4770K; RAM: 16 GB). The key simulation parameters are presented in Table 2. The vehicle arrival rate follows the Poisson distribution and the average arrival rate λ varies between 0.1 and 0.25 veh/s. It should be noted that when the arrival rates from both legs are $>0.25 \text{ veh/s}$, the traffic becomes very congested and most vehicles start to back up towards the upstream.

6.1 Microscopic impact on traffic flow characteristics

Fig. 9a shows the vehicle trajectories of on-ramp merging with 100% human-driven vehicles. Since there are no interactions between human-driven vehicles before the pre-merging zone, the ramp vehicles will yield to the main road vehicles near the merging zone, which causes stop-and-go operations. Worse, the shockwave will propagate to the upstream on the ramp road. Fig. 9b shows the trajectories of partial coordination between CAVs and non-CAVs and it clearly reveals how the CAVs harmonise traffic flow dynamics. The position and velocity of the main road vehicle can be measured by its preceding CAV, thus, the ramp road CAV can adjust its arrival time to avoid the excessive brake near the merging zone. In other words, partial coordination makes the trajectories

smoother and mitigates the shockwaves.

Further, Fig. 10 shows the velocity profiles in both no coordination and partial coordination cases. As expected, without coordination, the on-ramp vehicles in Fig. 10a execute excessive brakes near the merging zone to avoid lateral collision with mainline vehicles. In contrast with Fig. 10b, partial coordination strategy and the motion planning method can effectively reduce the speed modulation and achieve speed harmonisation, which makes the velocity profiles smoother. Moreover, comparing the two sets of results, we can see that the partial coordination of CAV can significantly smooth not only the CAV trajectory but also the trajectories of vehicles following the CAV.

Moreover, the spatial-temporal diagram is utilised to show the microscopic impact of CAV penetration on traffic flow. Figs. 11a–d represent the spatial-temporal diagrams under CAV penetration 0, 30, 70 and 100%, respectively. The trajectories in Fig. 11a show that there are obvious stop-and-go operations under the merging process of 100% non-CAVs and the shockwaves will be propagated to the upstream, which causes traffic congestion.

From Figs. 11b–d, the stop-and-goes are gradually mitigated with the increase of CAV penetrations. Since CAVs can adjust their arrival time at the merging zone according to the estimated arrival time of non-CAVs, they can avoid excessive interaction with non-CAVs within the merging zone. The stop-and-go operations may only occur in the case of two non-CAVs merging from two legs. In particular, all the vehicles can pass the merging zone smoothly and efficiently under 100% CAV penetration. Thus, the proposed cooperative merging strategies can effectively mitigate traffic congestion with about 30% CAV penetration under mixed traffic scenarios.

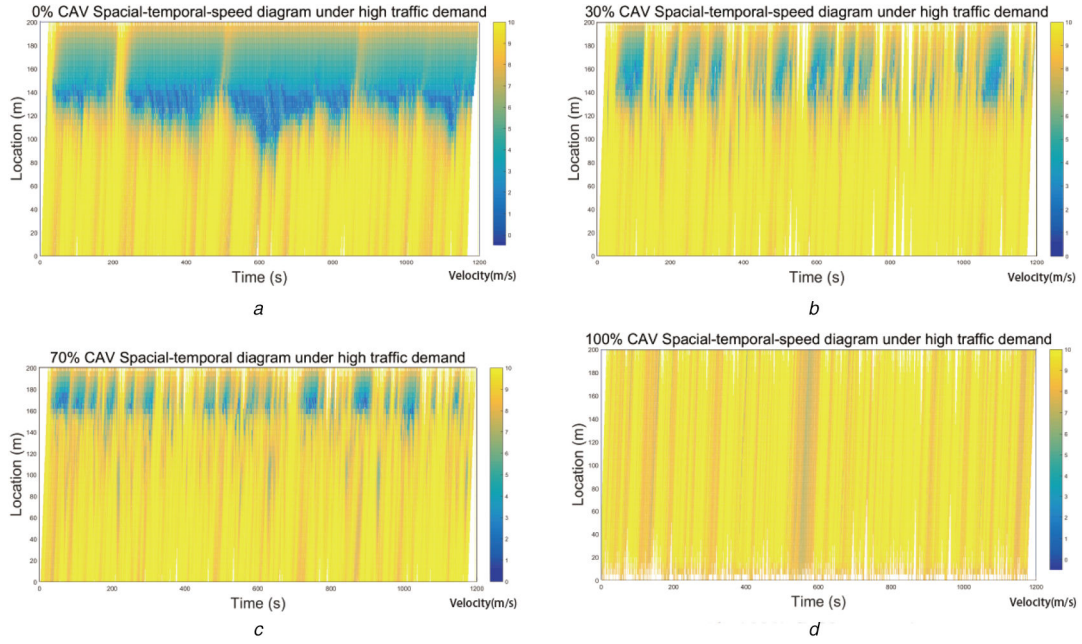


Fig. 11 Spatial-temporal diagram of cooperative merging under different CAV penetrations
(a) 0% CAV penetration, (b) 30% CAV penetration, (c) 70% CAV penetration, (d) 100% CAV penetration

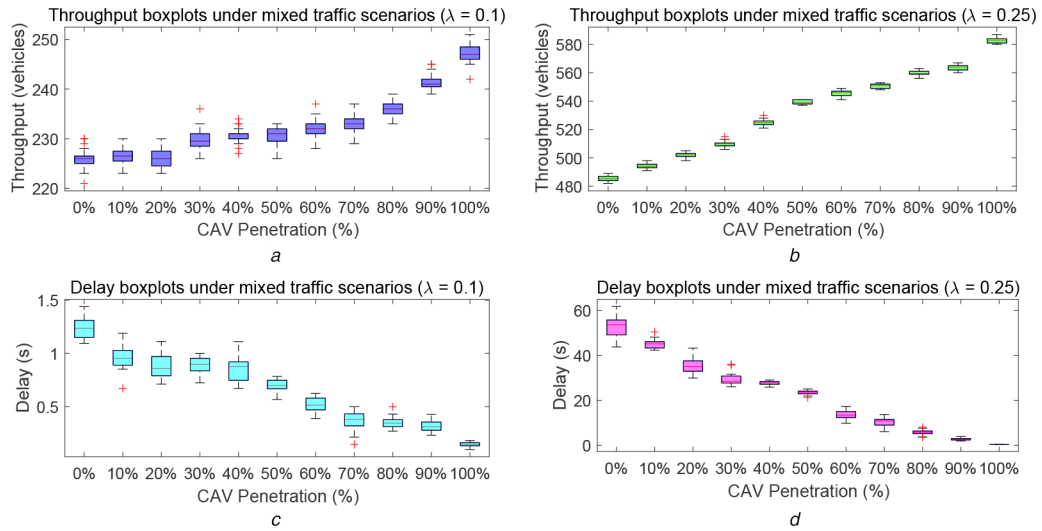


Fig. 12 Throughput and delay under different CAV penetrations and different vehicle arrival rates
(a) Throughput under low traffic demand, (b) Throughput under high traffic demand, (c) Delay under low traffic demand, (d) Delay under high traffic demand

6.2 Macroscopic impact on traffic flow characteristics

A simulation-based case study is carried out to validate the benefits of CAV penetration under mixed traffic scenarios. Throughput, delay, fuel consumption, emission and velocity deviation are utilised to evaluate the macroscopic performance under different CAV penetrations and different vehicle arrival rates (e.g. low traffic demand and high traffic demand).

Delay is measured by the difference between the actual passing time and the minimum passing time [7]. To quantify the benefits in terms of energy, a polynomial model estimating fuel consumption of a vehicle in [28] is adopted, which takes instantaneous velocity and acceleration as inputs. Further, VT-Micro model [29] is selected for measuring the emission during the cooperative merging process. Velocity standard deviation [15] is an indicator of velocity variation which may cause passengers' dissatisfaction.

Figs. 12a and b show the penetration effect on throughput under different vehicle arrival rates. Under low traffic demand (i.e. $\lambda = 0.1$ veh/s), the throughput benefits of CAVs are limited when the CAV penetration is $<30\%$. The reason lies in that the behaviours of some of the CAVs are limited by the human-driven vehicles which have to stop on the ramp and wait for a gap to merge. In general, with the increase of CAV penetration, the

average throughput is improved by the cooperative merging strategies of CAVs. In addition, the benefits of CAV coordination become more significant under high traffic demand, e.g., comparing results under 0 and 100% CAV penetration, throughput is improved by 9.8% under vehicle arrival rates 0.1 veh/s while the improvement is about 20% under vehicle arrival rates 0.25 veh/s.

As expected, a descending trend of delay can be witnessed when penetration rate keeps increasing in Figs. 12c and d. In particular, the average delay is reduced by about 45% when the penetration rate of CAVs reaches about 30%. Since the coordination strategies assign arrival time to the CAVs according to the estimated information of non-CAVs, there is less interaction with human-driven vehicles within the merging zone. Namely, the CAVs can adjust their velocity in advance to avoid the stop-and-goes during the merging process, which causes less delay. Under high traffic demand (i.e. $\lambda = 0.25$ veh/s), the congestion becomes serious with low CAV penetration and the average delay can be reduced by nearly half with about 50% of CAV penetration. The decreasing trend is relatively steep when the CAV penetration ranges from 50 to 100%, which means that the majority of CAVs work in a full coordination mode to reduce the travel delay. Under high CAV penetrations, the coordination policy makes better use of

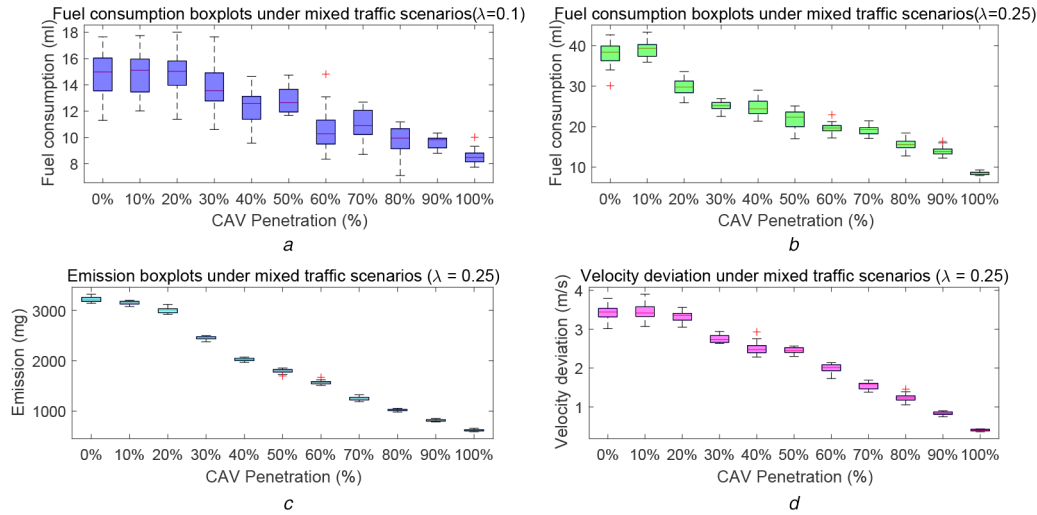


Fig. 13 Fuel consumption, emission and velocity deviation under different CAV penetrations and different vehicle arrival rates

(a) Fuel consumption under low traffic demand, (b) Fuel consumption under high traffic demand, (c) Emission under high traffic demand, (d) Velocity deviation under high traffic demand

the cooperative control zone, which reduces the travel delay during the merging process.

To explore the energy impact of CAV penetration with different traffic demands, a comparison is presented in Figs. 13a and b that shows the fuel consumption with respect to both different CAV penetration rates and vehicle arrival rates. The improvement in fuel consumption is limited, with CAV penetration <40% under low traffic demand. Since when the CAV penetration is low, the majority of CAVs are operated in the adaptive cruising mode, which consumes more energy than the free driving mode. Statistically, the fuel consumption can be reduced by nearly half with the CAV penetration of 50–60%. When the traffic is heavy, both CAVs and non-CAVs need to slow down or even stop to yield when they approach the merging zone without coordination and accelerate after they pass the merging zone, which may consume more energy compared to the scenario of light traffic.

A similar trend can be found in the results of emission and the standard deviation of velocity, as shown in Figs. 13c and d. The decreasing trend in Fig. 13c is relatively steep when penetration rate rises from 40 to 70%, which means CAVs can contribute more to reduce emission if they are the majority of vehicles. When the human-driven vehicles are the major part, CAVs have to give priorities to them frequently; thus, the collaboration that CAVs provided is relatively limited. With more CAVs, the total travel time can be reduced with the cooperative merging framework and hence reduce the emission. When the penetration rate reaches a relatively high level, most of the disturbances are able to be avoided at high level (80%) of penetration rate in Fig. 13d. As aforementioned in the microscopic impact part, CAVs can decelerate with a relatively low deceleration rate to avoid passengers' dissatisfaction while avoiding the lateral collision at the same time. Hence, disturbances cumulated along the traffic flow, which causes shockwave, can be effectively avoided and the velocity standard deviation can be reduced to enhance ride comfort of passengers. Statistically, about 30–40% CAV penetration can effectively reduce the velocity standard deviation by half under light traffic (e.g. $\lambda \leq 0.15$ veh/s), while it needs about 60–70% CAV penetrations to achieve the same performance under heavy traffic (e.g. $\lambda \geq 0.2$ veh/s).

7 Conclusion

In this paper, we propose a hierarchical coordination framework for on-ramp merging under mixed traffic scenarios, which is different from our earlier work under 100% CAV environment. In addition, we investigate both microscopic impacts and macroscopic impacts of CAV penetration on the merging performance under different traffic demands. Simulation-based case studies indicate that the improvement in throughput, delay and fuel consumption can be increased by up to 4.9, 45.9 and 34.7%, respectively, under 30%

CAV penetration. The benefits become more significant as the CAV penetration rate increases, which provide strong evidence of the advantages of incorporating CAVs into current traffic systems.

Future works should investigate the scenario of mainline with multiple lanes, where both cooperative lane-changing and cooperative merging should be taken into consideration. Furthermore, some computational intelligence assisted design approaches [30] combined with some heuristic rules [31] should also be investigated.

8 Acknowledgments

This work was supported in part by the National Natural Science Foundation of China under grant no. 61673233, Beijing Municipal Science and Technology Program under grant D171100004917001/2, National 13-5 Key R&D Program Projects under grant no. 2018YFB160 0600.

9 References

- [1] Mizuta, A., Roberts, K., Jacobsen, L., et al.: 'Ramp metering: a proven, cost-effective operational strategy – a primer'. Technical report, 2014
- [2] Agarwal, S., Kachroo, P., Contreras, S., et al.: 'Feedback-coordinated ramp control of consecutive on-ramps using distributed modeling and Godunov-based satisfiable allocation', *IEEE Trans. Intell. Transp. Syst.*, 2015, **16**, (5), pp. 2384–2392
- [3] Kotsialos, A., Papageorgiou, M.: 'Nonlinear optimal control applied to coordinated ramp metering', *IEEE Trans. Control Syst. Technol.*, 2004, **12**, (6), pp. 920–933
- [4] Papamichail, I., Papageorgiou, M.: 'Traffic-responsive linked ramp-metering control', *IEEE Trans. Intell. Transp. Syst.*, 2008, **9**, (1), pp. 111–121
- [5] Li, L., Wen, D., Yao, D.: 'A survey of traffic control with vehicular communications', *IEEE Trans. Intell. Transp. Syst.*, 2014, **15**, (1), pp. 425–432
- [6] Li, L., Wang, F.-Y.: 'Cooperative driving at blind crossings using intervehicle communication', *IEEE Trans. Veh. Technol.*, 2006, **55**, (6), pp. 1712–1724
- [7] Ding, J., Li, L., Zhang, Y., et al.: 'A rule-based cooperative vehicle merging strategy for connected and automated vehicles', *IEEE Trans. Intell. Transp. Syst.*, 2019, pp. 1–11, DOI: 10.1109/TITS.2019.2928969
- [8] James, R.M., Melson, C., Hu, J., et al.: 'Characterizing the impact of production adaptive cruise control on traffic flow: an investigation', *Transportmetrica B: Transp. Dyn.*, 2019, **7**, (1), pp. 992–1012
- [9] Rios-Torres, J., Malikopoulos, A.A.: 'Automated and cooperative vehicle merging at highway on-ramps', *IEEE Trans. Intell. Transp. Syst.*, 2017, **18**, (4), pp. 780–789
- [10] Meng, Y., Li, L., Wang, F.-Y., et al.: 'Analysis of cooperative driving strategies for nonsignalized intersections', *IEEE Trans. Veh. Technol.*, 2018, **67**, (4), pp. 2900–2911
- [11] Xu, H., Feng, S., Zhang, Y., et al.: 'A grouping based cooperative driving strategy for CAVs merging problems', *IEEE Trans. Veh. Technol.*, 2019, **68**, pp. 6125–6136
- [12] Rios-Torres, J., Malikopoulos, A.A.: 'A survey on the coordination of connected and automated vehicles at intersections and merging at highway on-ramps', *IEEE Trans. Intell. Transp. Syst.*, 2017, **18**, (5), pp. 1066–1077
- [13] Zhang, Y., Cassandras, C.G.: 'The penetration effect of connected automated vehicles in urban traffic: an energy impact study', arXiv preprint arXiv:1803.05577, 2018, pp. 1–8

- [14] Zhao, L., Malikopoulos, A., Rios-Torres, J.: 'Optimal control of connected and automated vehicles at roundabouts: an investigation in a mixed-traffic environment', *IFAC-PapersOnLine*, 2018, **51**, (9), pp. 73–78
- [15] Zou, Y., Qu, X.: 'On the impact of connected automated vehicles in freeway work zones: a cooperative cellular automata model based approach', *J. Intell. Connect. Veh.*, 2018, **1**, (1), pp. 1–14
- [16] Zhou, M., Qu, X., Jin, S.: 'On the impact of cooperative autonomous vehicles in improving freeway merging: a modified intelligent driver model-based approach', *IEEE Trans. Intell. Transp. Syst.*, 2016, **18**, (6), pp. 1422–1428
- [17] Park, H., Bhamidipati, C.S., Smith, B.L.: 'Development and evaluation of enhanced intellidrive-enabled lane changing advisory algorithm to address freeway merge conflict', *Transp. Res. Rec.*, 2011, **2243**, (1), pp. 146–157
- [18] Han, Y., Ahn, S.: 'Variable speed release (VSR): speed control to increase bottleneck capacity', *IEEE Trans. Intell. Transp. Syst.*, 2019, pp. 1–10, DOI: 10.1109/TITS.2019.2891314
- [19] Davis, L.C.: 'Effect of adaptive cruise control systems on mixed traffic flow near an on-ramp', *Physica A, Stat. Mech. App.*, 2007, **379**, (1), pp. 274–290
- [20] Rios-Torres, J., Malikopoulos, A.A.: 'Energy impact of different penetrations of connected and automated vehicles: a preliminary assessment'. Proc. of the 9th ACM SIGSPATIAL Int. Workshop on Computational Transportation Science, Burlingame, CA, USA, 31 October–3 November 2016, pp. 1–6
- [21] Rios-Torres, J., Malikopoulos, A.A.: 'Impact of partial penetrations of connected and automated vehicles on fuel consumption and traffic flow', *IEEE Trans. Intell. Veh.*, 2018, **3**, (4), pp. 453–462
- [22] Bai, Y., Zhang, Y., Li, X., *et al.*: 'Cooperative weaving for connected and automated vehicles to reduce traffic oscillation', *Transportmetrica A: Transp. Sci.*, 2019, **1225**, pp. 1–19
- [23] Xie, Y., Zhang, H., Gartner, N.H., *et al.*: 'Collaborative merging strategy for freeway ramp operations in a connected and autonomous vehicles environment', *J. Intell. Transp. Syst.*, 2017, **21**, (2), pp. 136–147
- [24] Letter, C., Elefteriadou, L.: 'Efficient control of fully automated connected vehicles at freeway merge segments', *Transp. Res. C, Emerg. Technol.*, 2017, **80**, pp. 190–205
- [25] Vinitsky, E., Kreidieh, A., Flem, L.L., *et al.*: 'Benchmarks for reinforcement learning in mixed-autonomy traffic'. Conf. on Robot Learning, Zürich, Switzerland, June 2018, pp. 399–409
- [26] Kreidieh, A.R., Wu, C., Bayen, A.M.: 'Dissipating stop-and-go waves in closed and open networks via deep reinforcement learning'. IEEE 2018 21st Int. Conf. on Intelligent Transportation Systems (ITSC), Maui, HI, USA, November 2018, pp. 1475–1480
- [27] Gipps, P.G.: 'A behavioural car-following model for computer simulation', *Transp. Res. B, Methodol.*, 1981, **15**, (2), pp. 105–111
- [28] Md Abdus, S.K., Masakazu, M., Junichi, M., *et al.*: 'Ecological vehicle control on roads with up-down slopes', *IEEE Trans. Intell. Transp. Syst.*, 2011, **12**, (3), pp. 783–794
- [29] Ahn, K., Rakha, H., Trani, A., *et al.*: 'Estimating vehicle fuel consumption and emissions based on instantaneous speed and acceleration levels', *J. Transp. Eng.*, 2002, **128**, (2), pp. 182–190
- [30] Chen, Y., Li, Y.: 'Computational intelligence assisted design: in industrial revolution 4.0' (CRC Press, Boca Raton, FL, USA, 2018)
- [31] Xu, H., Zhang, Y., Li, L., *et al.*: 'Cooperative driving at unsignalized intersections using tree search', *IEEE Trans. Intell. Transp. Syst.*, 2019, pp. 1–9, accepted